

# Anomalous Raman shift in the ternary fullerenes with $t_{1g}$ states

X. H. Chen

*Japan Advanced Institute of Science and Technology*

*Tatsunokuchi, Ishikawa 923-1292, Japan*

*and Department of Physics, University of Science and Technology of China*

*Hefei, Anhui 230026, P. R. China*

T. Takenobu, T. Muro, H. Fudo, and Y. Iwasa

*Japan Advanced Institute of Science and Technology*

*Tatsunokuchi, Ishikawa 923-1292, Japan*

(February 3, 1999)

## Abstract

Raman spectra have been studied on two kinds of highly doped fullerenes of  $A_xBa_3C_{60}$  ( $x=0, 3$ ;  $A=K, Rb$ ) and  $K_xSm_{2.75}C_{60}$  ( $x=0, 3.25$ ). It was found that the Raman spectra are essentially identical to each other for all ternary fullerenes. The results show a crossover point at the boundary of  $t_{1u}$  and  $t_{1g}$  bands for the charge transfer dependence of Raman shift. Particularly, the totally symmetric  $A_g(2)$  mode in  $t_{1g}$  fullerenes cannot be understood by a simple extrapolation from the low doped  $t_{1u}$  fullerenes, where the  $A_g(2)$  mode follows a characteristic shift of  $\sim 6.3cm^{-1}$  per elementary charge. The present result shows that the Raman spectra of  $t_{1g}$  states cannot be explained only by charge transfer.

**PACS numbers: 78.30.-j, 72.80.Rj, 74.70.-b**

Raman scattering is a useful technique to study the vibrational properties of the  $C_{60}$  molecule and its doped derivative compounds. Raman scattering is widely used to evaluate the electron-phonon coupling constant  $\lambda$  for the doped  $C_{60}$  superconductors basing on the analysis of the linewidths.<sup>1-3</sup> In addition, the tangential pinch  $A_g(2)$  mode is of particular interest in the studies of the doped  $C_{60}$  as it yields a strong and narrow line in the Raman spectrum. The different stages of doping can be easily followed by in-situ Raman-scattering experiments. A continuous change of line intensity for the  $A_g(2)$  mode of the stable phase is observed and the doping process leads to a characteristic downshift of this line regarding the number of electrons transferred to the  $C_{60}$  molecule. A down-shift of 6-7  $cm^{-1}$  per elementary charge on  $C_{60}$  independent of the doping ion is observed.<sup>4-8</sup> The  $AC_{60}$  phase was discovered by down-shift of the  $A_g$  pinch mode in in-situ Raman-scattering experiments.<sup>9</sup>

$A_3Ba_3C_{60}$  phases (A=K, Rb, Cs) with a formal  $C_{60}^{-9}$  charge and half-filling of the  $t_{1g}$  are recently reported.<sup>10</sup> As the intercalation host,  $Ba_3C_{60}$  is a vacancy-ordered derivative of the bcc  $A_6C_{60}$  structure with half of the cation sites empty (A15 structure). Three alkali metal cations are introduced into  $Ba_3C_{60}$  to form a cation-disordered  $A_3Ba_3C_{60}$  phase isostructural with  $A_6C_{60}$ .  $K_3Ba_3C_{60}$  with half-filled  $t_{1g}$  band exhibits superconductivity at 5.6 K. However, the insertion of large  $A^+$  cations leads to a decrease in  $T_c$ , contrary to the behavior of the  $A_3C_{60}$  phases.<sup>11</sup>

To investigate the vibrational properties of ternary fullerides and comparison of physical properties in between  $t_{1u}$  and  $t_{1g}$  fullerides, we have carried out a Raman scattering study on the fullerides  $A_xBa_3C_{60}$  (x=0, 3; A=K, Rb) and  $K_xSm_{2.75}C_{60}$  (x=0, 3.25). The results show that the Raman spectra are amazingly similar to each other for all ternary fullerides  $A_3Ba_3C_{60}$  and  $K_{3.25}Sm_{2.75}C_{60}$ . An anomalous Raman shift of the two  $A_g$  modes is observed when alkali metals are introduced into  $Ba_3C_{60}$  and  $Sm_{2.75}C_{60}$ . It does not follow the characteristic relation between charge transfer and Raman shift widely observed for the two  $A_g$  modes in alkali and Ca-doped  $C_{60}$ .<sup>4-7,12</sup>

Samples of  $Ba_3C_{60}$  and  $Sm_{2.75}C_{60}$  were synthesized by reacting stoichiometric amount of powers of Ba, Sm, and  $C_{60}$ . A quartz tube with mixed powder inside was sealed under high

vacuum of about  $2 \times 10^{-6}$  torr, and heated at  $550 \sim 600$  °C for three days. Synthesis of  $A_3Ba_3C_{60}$  and  $K_{3.25}Sm_{2.75}C_{60}$  was carried out in a similar manner to that of alkali doping into pure  $C_{60}$ . A piece of alkali and  $Ba_3C_{60}$  or  $Sm_{2.75}C_{60}$  powders were loaded in a Pyrex tube, which was sealed under  $2 \times 10^{-6}$  torr and calcined at 250 °C for three days. X-ray diffraction analysis was performed by a system equipped with a 4.5 kW rotating molybdenum anode as the x-ray generator and an imaging plate (IP, MAC, Science , DIP320V ) as the detector. X-ray diffraction showed that all samples were single phase, which was also confirmed by the single peak feature of the pentagonal pinch  $A_g(2)$  mode in the Raman spectra.

Raman scattering experiments were carried out using the 632.8 nm line of a He-Ne laser in the Brewster angle backscattering geometry. The scattering light was detected with a Dilor xy multichannel spectrometer using a spectral resolution of  $3\text{ cm}^{-1}$ . In order to obtain good Raman spectra, the samples were ground and pressed into pellets with pressure of about  $20\text{ kg/cm}^2$ , which were sealed in Pyrex tubes under a high vacuum of  $10^{-6}$  torr.

As reported in reference 10, X-ray diffraction shows that the structure is changed from  $A15$  phase to a cation-disordered  $A_3Ba_3C_{60}$  phase isostructural with bcc  $A_6C_{60}$  ( $a=K, Ba$ ) when alkali metal is intercalated into  $Ba_3C_{60}$ . Figure 1 shows the X-ray powder diffraction patterns for the samples  $Sm_{2.75}C_{60}$  and  $K_{3.25}Sm_{2.75}C_{60}$ . For the pattern of  $Sm_{2.75}C_{60}$ , all peaks can be indexed with an orthorhombic lattice parameters  $a=28.158\text{ \AA}$ ,  $b=28.077\text{ \AA}$ , and  $c=28.270\text{ \AA}$ , which is consistent with previous report.<sup>13</sup> It is easily seen in Fig.1 that the diffraction peak is much less in the pattern of  $K_{3.25}Sm_{2.75}C_{60}$  than in the pattern of  $Sm_{2.75}C_{60}$ . In addition, no peak is observed at  $2\theta$  below 5 degree. It suggests that the structure of  $K_{3.25}Sm_{2.75}C_{60}$  should be simple relative to that of  $Sm_{2.75}C_{60}$ . We can index all diffraction peaks using a body-center ed-cubic cell with lattice parameter  $a=11.093\text{ \AA}$  except for the two peaks marked by arrows in Fig.1. It is known that the basic structure of  $Sm_{2.75}C_{60}$  is fcc, but the cation vacancy ordering in tetrahedral sites leads to a superstructure accompanied with a slight lattice deformation from cubic to orthorhombic. The Sm cations occupying the octahedral and tetrahedral sites experience off-center displacements since one out of every eight tetrahedral sites in the subcell is vacant.<sup>13</sup> X-ray diffraction

suggests that introduction of the alkali cations into  $Sm_{2.75}C_{60}$  leads to the disappearance of cation-vacancy ordering and formation of a cation-disordered phase with composition  $K_{3.25}Sm_{2.75}C_{60}$ , similarly to the case of  $A_3Ba_3C_{60}$ . A detailed analysis on the structure of  $K_{3.25}Sm_{2.75}C_{60}$  will be reported elsewhere.

Figure 2 shows Raman spectra of  $Ba_3C_{60}$ ,  $K_3Ba_3C_{60}$ , and  $Rb_3Ba_3C_{60}$ . The positions (  $\omega$  ) and halfwidths (  $\gamma$  ) of the Raman modes observed are listed in Table I for all samples. In the  $Ba_3C_{60}$  spectrum, there are about 13 strong Raman lines observed, some of which are doublets. The low-and high-frequency  $A_g$  derived modes are located at 506 and 1430.8  $cm^{-1}$ , respectively. The position of  $A_g(2)$  pentagonal pinch mode is identical to that of  $K_6C_{60}$ , suggesting that the charge transfer from Ba to  $C_{60}$  is complete, also being consistent with  $\sim 6.3 cm^{-1}$  redshift per electron relative to neutral  $C_{60}$ .<sup>8</sup> However, the up-shift of 13  $cm^{-1}$  for the radial  $A_g(1)$  mode is larger than that for  $K_6C_{60}$  (9  $cm^{-1}$ ).<sup>14</sup> It is to be pointed out that the Raman spectrum of  $Ba_3C_{60}$  is amazingly similar to that of  $K_6C_{60}$  except for the relative intensities between  $A_g(2)$  and  $H_g(2)$  modes.

In the case of  $K_3Ba_3C_{60}$  and  $Rb_3Ba_3C_{60}$ , the similar Raman lines to  $Ba_3C_{60}$  are observed. However, the strongest line is  $A_g(2)$  mode, similarly to the case of  $K_6C_{60}$  with bcc structure. It is worth pointing out that the  $K_3Ba_3C_{60}$  and  $Rb_3Ba_3C_{60}$  spectra are essentially identical to each other. These spectra are relatively insensitive to the choice of alkali-metal ion species. This behavior is similar to the case of  $A_3C_{60}$  and  $A_6C_{60}$  ( A=K, Rb ) compounds, where this behavior is explained both by a weak coupling between  $C_{60}$  and alkali cations and by a complete charge transfer from the alkali-metals to  $C_{60}$  molecules.<sup>14</sup> However, an anomalous Raman shift for the two  $A_g$ -derived modes is observed in  $K_3Ba_3C_{60}$  and  $Rb_3Ba_3C_{60}$ . The first thing to be noted is the  $A_g(2)$  mode observed at 1425.5 ( 1424.1 )  $cm^{-1}$  in  $K_3Ba_3C_{60}$  ( $Rb_3Ba_3C_{60}$ ). The relative down-shift of  $A_g(2)$  mode measured from that of  $Ba_3C_{60}$  is only 5.3 and 6.7  $cm^{-1}$  for  $K_3Ba_3C_{60}$  and  $Rb_3Ba_3C_{60}$ , respectively. These values are much smaller than that expected basing on the established empirical relation between the formal  $C_{60}$  valence and the Raman shift. Another anomaly is found in the radial  $A_g(1)$  mode, which shows a downshift of 8.6 and 10.5  $cm^{-1}$  relative to  $Ba_3C_{60}$  for  $K_3Ba_3C_{60}$  ( $Rb_3Ba_3C_{60}$ ),

respectively. Such a large downshift upon alkali metal doping displays a sharp contrast with the case of  $A_xC_{60}$  (A=K, Rb) where a slight upshift is observed with increasing alkali metal. Low frequency  $H_g$  modes also show complicated and characteristic behavior. The  $H_g(2)$  mode of cubic  $Ba_3C_{60}$  is single peak at  $432\text{ cm}^{-1}$ , while it shows a splitting into two peaks both in  $K_3Ba_3C_{60}$  and  $Rb_3Ba_3C_{60}$ . The splitting of  $H_g(3)$  mode is observed in all samples in Fig.2, and the splitting is smaller in the alkali-doped ternaries, while the center of doublet remains unchanged. .

Room temperature Raman spectra of the samples  $Sm_{2.75}C_{60}$  and  $K_{3.25}Sm_{2.75}C_{60}$  are shown in Fig.3. For  $Sm_{2.75}C_{60}$ , an anomalously broad distribution of vibrational structures for the low frequency  $H_g$  modes and around the  $A_g(2)$  mode is observed, which could be related to the complexity of  $Sm_{2.75}C_{60}$  structure. The low frequency  $H_g(1)$  and  $H_g(2)$  modes are asymmetric.  $H_g(2)$  mode has to be fitted with four components. It suggests that the degeneracy  $H_g(2)$  mode is lifted. This splitting may be attributed to the symmetry lowering due to the orthorhombic superstructure of this material. A similar behavior has been observed in single crystal  $K_3C_{60}$  at 80 K<sup>3</sup> and in  $Ba_4C_{60}$  and  $Ba_6C_{60}$  at room temperature.<sup>15</sup> A bunch of lines appears around  $700\text{ cm}^{-1}$  which are likely to be assigned to the  $H_g(3)$  and  $H_g(4)$  modes. It is to be pointed out that the pinch  $A_g(2)$  mode occurs at  $1432.8\text{ cm}^{-1}$ , indicating that Sm is divalent, and the charge transfer is complete according to  $6.3\text{ cm}^{-1}$  redshift per electron relative to neutral  $C_{60}$ . The position of the radial  $A_g(1)$  is also consistent with that of  $A_6C_{60}$  (A=K, Rb).<sup>14</sup> This definitely confirms divalent Sm by Raman scattering, being consistent with the results of near-edge and extended X-ray absorption fine structure in  $Yb_{2.75}C_{60}$ .<sup>17</sup>

The top of Fig.3 shows the spectrum of  $K_{3.25}Sm_{2.75}C_{60}$ , which is amazingly similar to  $A_3Ba_3C_{60}$  although the Raman spectra of the intercalation host materials are different. Table I shows that even the positions of all corresponding modes are almost the same between  $K_{3.25}Sm_{2.75}C_{60}$  and  $A_3Ba_3C_{60}$  compounds. This surprising result strongly indicates that Raman spectrum is insensitive to the metal ion species either in the intercalation host or as an intercalation guest, suggesting a weak coupling between the  $C_{60}$  and the metal ions and

a complete charge transfer from metal cations to  $C_{60}$  molecules.

Raman shift of the radial  $A_g(1)$  and  $A_g(2)$  pinch modes as a function of the nominal charge transfer simply derived from the chemical formula for  $Ba_3C_{60}$ ,  $Sm_{2.75}C_{60}$ ,  $A_3Ba_3C_{60}$  ( $A=K, Rb$ ), and  $K_{3.25}Sm_{2.75}C_{60}$  are plotted in Fig.4. For comparison, the results of  $Ba_xC_{60}$  ( $x=4, 6$ ) recently reported by us<sup>15</sup>,  $K_xC_{60}$  ( $x=3, 6$ ) reported by Duclos et al.<sup>5</sup>, and  $KBa_2C_{60}$  and  $KBaCs_{60}$  reported by Yildirim et al.<sup>16</sup> are also plotted in the figure. For the  $A_g(2)$  mode, there is a boundary at charge transfer of 6 electrons. Below which, the relation between the Raman shift of  $A_g(2)$  mode and charge transfer is linear. They follow the characteristic shift of  $\sim 6.3 \text{ cm}^{-1}$  redshift per elementary charge for the all samples including  $Ba_3C_{60}$  and  $Sm_{2.75}C_{60}$ . However, when the charge transfer exceeds six, the pinch  $A_g(2)$  mode does not follow the simple characteristic relation, showing a complicated behavior. In other words, although there exist a systematic relation between Raman shift and charge transfer for the " $t_{1u}$  band" fullerides, the " $t_{1g}$  band" fullerides are quite different. The charge transferred from metal to  $C_{60}$  molecules were -9, -15, and -7 for the  $Ba_4C_{60}$ ,  $Ba_6C_{60}$ , and  $K_3Ba_3C_{60}$  ( $K_{3.25}Sm_{2.75}C_{60}$ ), respectively, if charge transfer was derived according to  $6.3 \text{ cm}^{-1}$  redshift per elementary charge. This is much larger ( less ) than the nominal charge transfer for  $Ba_xC_{60}$  ( $x=4$  and  $6$ ) ( $K_3Ba_3C_{60}$  and  $K_{3.25}Sm_{2.75}C_{60}$ ). If the charge transfer from Ba to  $C_{60}$  molecules is complete, the redshift per elementary charge is about  $9 \text{ cm}^{-1}$ , being much larger than  $\sim 6.3 \text{ cm}^{-1}$ . In addition, an anomalous Raman shift for the  $A_g$  derived modes takes place in the ternary  $A_3Ba_3C_{60}$  ( $A=K, Rb$ ) and  $K_{3.25}Sm_{2.75}C_{60}$ , the down-shift is only about  $6 \text{ cm}^{-1}$  for the nominal charge transfer of three electrons relative to  $Ba_3C_{60}$  and  $Sm_{2.75}C_{60}$ .

Let us switch to the arguments on the radial  $A_g(1)$  mode. A continuous up-shift of the  $A_g(1)$  mode with increasing charge transfer until six electrons observed as shown in Fig.4. This mode-stiffening has been explained by electrostatic interactions which produces sufficient stiffening to encounter the softening of the mode expected on the basis of charge transfer effects.<sup>18,12</sup> It is to be noted that the Raman shift of the radial  $A_g(1)$  for  $Sm_{2.75}C_{60}$  with  $t_{1u}$  states falls on the linear line of  $K_xC_{60}$  with  $t_{1u}$  states. In contrast, in the  $t_{1g}$  fullerides, the frequency of the  $A_g(1)$  mode almost remains unchanged for  $Ba_xC_{60}$ , while

it decreases with increasing charge transfer in the ternaries  $A_3Ba_3C_{60}$  and  $K_{3.25}Sm_{2.75}C_{60}$ . It is worth noting that both  $A_g(1)$  and  $A_g(2)$  modes show complicated behavior in the  $t_{1g}$  bands.

In the case of Ba derived fullerenes, a strong hybridization between the Ba atoms and the  $\pi$ -type functions of the  $C_{60}$  network<sup>19–21</sup> may be responsible for the behavior of the  $A_g$  derived modes as discussed in Ref.15. The charge transfer is complete in the intercalation hosts of  $Ba_3C_{60}$  and  $Sm_{2.75}C_{60}$ , following the characteristic relation between Raman shift and charge transfer, while the introduction of alkali metals leads to an anomalous Raman shift for the two  $A_g$  derived modes in the ternary  $A_3Ba_3C_{60}$  and  $K_{3.25}Sm_{2.75}C_{60}$ . However, the Raman shift of  $A_g(2)$  pinch mode follows the characteristic shift of  $\sim 6.3 \text{ cm}^{-1}$  per elementary charge transfer for the co-intercalated  $C_{60}$  of  $ABa_2C_{60}$  ( $A=K, Rb, \text{ and } Cs$ ) and  $KBaCsC_{60}$  with  $t_{1u}$  states.<sup>16</sup> It suggests that the anomalous Raman shift of the  $A_g$  mode could be related to the " $t_{1g}$ " band electrons. In fact, some other differences between the " $t_{1u}$ " and " $t_{1g}$ " superconductors have been found. In the  $t_{1u}$  band, superconductivity occurs only at  $(C_{60})^{-3}$  state which corresponds to the half-filling of the  $t_{1u}$  band.<sup>22</sup> However, the reported " $t_{1g}$ " superconductors are  $B_4C_{60}$  ( $B=Ba, Sr$ ),  $A_3Ba_3C_{60}$ , and  $Ca_5C_{60}$ . which have the molecular valences of -8, -9, and -10, respectively. Such tolerance for the molecular valence in  $t_{1g}$  superconductor makes a striking contrast with the strict constraint for the valence state in the case of " $t_{1u}$ " superconductors. Another difference to be pointed out is that the " $t_{1u}$ " superconductivity appears only in fcc or related structures. In the case of  $t_{1g}$  band, superconductivity is observed in various structures, even orthorhombic structure. To completely understand the physical properties and superconducting mechanism of fullerenes, it is necessary to further investigate  $t_{1g}$  fullerenes, and to explain the difference between  $t_{1u}$  and  $t_{1g}$  fullerenes.

In summary, the Raman scattering study has been carried out in the two fullerene families of  $A_xBa_3C_{60}$  ( $x=0, 3$ ;  $A=K, Rb$ ) and  $K_xSm_{2.75}C_{60}$  ( $x=0, 3.25$ ). The results definitely show some differences between  $t_{1u}$  and  $t_{1g}$  fullerene for Raman shift of the two  $A_g$  modes. For  $t_{1u}$  fullerenes, the down-shift of the  $A_g(2)$  mode and the up-shift of  $A_g(1)$  mode can be explained

by charge transfer and the electrostatic interactions upon doping, respectively. In contrast, the  $t_{1g}$  fullerides show a complicated behavior for Raman shift of the two  $A_g$  modes. The Raman shifts of the two  $A_g$  modes, observed in the ternaries  $A_3Ba_3C_{60}$  and  $K_{3.25}Sm_{2.75}C_{60}$ , significantly differ from that of the binary fullerides  $Ba_4C_{60}$  and  $Ba_6C_{60}$ . It is also found that Raman spectra of  $A_3Ba_3C_{60}$  and  $K_{3.25}Sm_{2.75}C_{60}$  are identical to each other, indicating a weak coupling between the  $C_{60}$  and metal cations, and the same charge transfer to  $C_{60}$  molecules. However, the anomalous Raman shift could not be explained only by the charge transfer.

X. H. Chen would like to thank the Inoue Foundation for Science for financial support. X. H. Chen acknowledges Dr. Kitagawa for his help in experiment. This work is partly supported by Grant from the Japan Society for Promotion of Science (RFTF 96P00104, MPCR-363/96-03262) and from the Ministry of Education, Science, Sports, and Culture.



## REFERENCES

- <sup>1</sup> M. G. Mitch, S. J. Chase and Lannin, Phys. Rev. Lett. **68**, 883(1992).
- <sup>2</sup> P. Zhou, K. A. Wang, P.C. Eklund, G. Dresselhaus, M.S. Dresselhaus, Phys. Rev. B **48**, 8412(1993).
- <sup>3</sup> J. Winter and H. Kuzmany Phys. Rev. B **53**, 655(1996).
- <sup>4</sup> R.C. Haddon, A.F. Hebbard, M.J. Rosseinsky, D.W. Murphy, A.J. Duclos, K.B. Lyons, B. Miller, J.M. Rosamilia, R.H. Fleming, A.R. Kortan, S.H. Glarum, A.V. Makhga, A.J. Muller, R.H. Eick, S.M. Zahurak, R.Tycko, G. Dabbah, and F. A. Thiel, Nature **350**, 320(1991).
- <sup>5</sup> S. J. Duclos, R. C. Haddon, S. H. Glarum, A. F. Hebbard and K. B. Lyons, Science **254**, 1625(1991).
- <sup>6</sup> T. Pichler, M.Matus, J.Kürti, and H. Kuzmany, Phys. Rev. B **45**, 13841(1992).
- <sup>7</sup> K.A. Wang, Y. Wang, P. Zhopu, J.M. Holden, S.L. Ren, G.T. Hager, H.F. Ni, P.C. Eklund, G. Dresselhaus, and M.S. Dresselhaus. Phys. Rev. B **45**, 1955(1992).
- <sup>8</sup> H. Kuzmany , M. Matus, B. Burger, and J. Winter, Adv. Mater. **6**, 731(1994).
- <sup>9</sup> J. Winter and H. Kuzmany, Solid State Commun. **84** 935(1992).
- <sup>10</sup> Y. Iwasa, H. Hayashi, T. Furudate, and T. Mitani, Phys. Rev. B **54**, 14960(1996).
- <sup>11</sup> Y. Iwasa, M. Kawaguchi, H. Iwasaki, T. Mitani, N. Wada, and T. Hasegawa Phys. Rev. B **57**, 13395(1998).
- <sup>12</sup> X.H. Chen, X. J. Zhou, and S. Roth, Phys. Rev. B **54**, 3971(1996).
- <sup>13</sup> X.H. Chen and G. Roth, Phys. Rev. B **52**, 15534(1995).
- <sup>14</sup> P. Zhou, K. A. Wang, Y. Wang, P. C. Eklund, M. S. Dresselhaus, G. Dresselhaus, R. A. Jishi Phys. Rev. B **46**, 2595(1992).

- <sup>15</sup> X.H. Chen, S. Taga, and Y. Iwasa, submitted to Phys. Rev. B
- <sup>16</sup> T. Yildirim, L. Barbedette, J.E. Fisher, G.M. Bendele, P.W. Stephens C.L. Lin, J. Robbert, P. Petit, and T.T.M. Palstra, Phys. Rev. B **54**, 11981(1996).
- <sup>17</sup> P.H. Citrin, E. Özdas, S. Schuppler , A.R. Kortan, and K.B. Lyons Phys. Rev. B **56**, 5213(1997).
- <sup>18</sup> R.A. Jishi and M.S. Dresselhauss, Phys. Rev. B **45**, 6914(1992).
- <sup>19</sup> S. Saito and A. Oshiyama, Phys. Rev. Lett. **71**, 121(1993).
- <sup>20</sup> S.C. Erwin and M.P. Pederson, Phys. Rev. B **47**, 14657(1993).
- <sup>21</sup> Th.S. Niederig, M.C. Böhm, H. Werner, J. Schlute, and R. Schlögl, Phys. rev. B **55**, 13542(1997).
- <sup>22</sup> T. Yildirim, L. Barbedette, J.E. Fisher, C.L. Lin, J. Robbert, P. Petit, and T.T.M. Palstra, Phys. Rev. Lett. **77**, 167(1996).

# TABLES

TABLE I. Positions and linewidths (in parentheses) for the Raman modes in  $Ba_3C_{60}$ ,  $A_3Ba_3C_{60}$  (A=K and Rb),  $Sm_{2.75}C_{60}$ , and  $K_{3.25}Sm_{2.75}C_{60}$

	$Ba_3C_{60}$	$K_3Ba_3C_{60}$	$Rb_3Ba_3C_{60}$	$Sm_{2.75}C_{60}$	$K_{3.25}Sm_{2.75}C_{60}$
$I_h$ mode	$\omega$ ( $\gamma$ )	$\omega$ ( $\gamma$ )	$\omega$ ( $\gamma$ )	$\omega$ ( $\gamma$ )	$\omega$ ( $\gamma$ )
	( $cm^{-1}$ )	( $cm^{-1}$ )	( $cm^{-1}$ )	( $cm^{-1}$ )	( $cm^{-1}$ )
$A_g(1)$	505.9 ( 4.2 )	497.3 ( 2.4 )	495.4 ( 3.7 )	498.3 ( 6.9 )	496.8 ( 5.0 )
$A_g(2)$	1430.8 ( 13.0 )	1425.5 ( 6.3 )	1424.1 ( 11.1 )	1432.8 ( 22.6 )	1424.7 ( 14.3 )
$H_g(1)$	273 ( 5.3 )	266.3 ( 11.9 )	266.6 ( 4.5 )	264.7 ( 23.3 )	265.6 ( 10.4 )
	278.7 ( 4.6 )	276.5 ( 3.0 )	272.8 ( 5.7 )	283.0 ( 3.1 )	276.0 ( 6.6 )
$H_g(2)$	432.3 ( 5.3 )	414.9 ( 2.3 )	417.8 ( 3.7 )	344.5 ( 38.3 )	415.0 ( 3.9 )
		422.9 ( 2.8 )	424.8 ( 2.9 )	400 ( 48.8 )	422.7 ( 18.0 )
				415.0 ( 18.0 )	
				427.0 ( 10.2 )	
$H_g(3)$	648.2 ( 8.5 )	653.5 ( 5.6 )	655.3 ( 5.8 )	647.9 ( 25.0 )	653.3 ( 7.2 )
	681.6 ( 7.8 )	673.3 ( 4.8 )	674.3 ( 4.2 )	683.4 ( 31.0 )	672.1 ( 12.9 )
$H_g(4)$	760.7 ( 8.4 )	757.7 ( 4.2 )	758.7 ( 5.6 )	756.7 ( 23.0 )	757.5 ( 7.8 )
$H_g(5)$	1091.7 ( 18.5 )	1086.0 ( 15.3 )	1086.7 ( 16.4 )	1085.5 ( 22.3 )	1088.0 ( 25.2 )
	1117.3 ( 12.8 )			1112.4 ( 12.8 )	
$H_g(6)$	1227.6 ( 16.1 )	1229.0 ( 9.8 )	1227.9 ( 13.1 )	1226.2 ( 20.9 )	1227.6 ( 16.7 )
$H_g(7)$	1322.1 ( 34.6 )	1314.0 ( 20.6 )	1315.5 ( 18.0 )		1317.9 ( 27.1 )
	1388.1 ( 15.3 )	1377.4 ( 8.9 )	1373 ( 23.5 )	1387 .8 ( 46 )	1378.2 ( 11.5 )
$H_g(8)$	1474.4 ( 26.1 )				

## FIGURE CAPTIONS

Figure 1:

Powder X-ray diffraction patterns of  $Sm_{2.75}C_{60}$  and  $K_{3.25}Sm_{2.75}C_{60}$ . The two peaks marked by arrows can not indexed with body-centered-cubic cell with lattice parameter  $a=11.093 \text{ \AA}$ .

Figure 2:

Room temperature Raman spectra of  $Ba_3C_{60}$ ,  $K_3Ba_3C_{60}$ , and  $Rb_3Ba_3C_{60}$ .

Figure 3:

Room temperature Raman spectra of  $Sm_{2.75}C_{60}$  and  $K_{3.25}Sm_{2.75}C_{60}$ .

Figure 4:

Charge transfer-Raman shift relation for the radial  $A_g(1)$  and  $A_g(2)$  pinch modes. Squares represent the current experimental results, circles refer to the experimental results of  $Ba_xC_{60}$  reported by us (Ref.15), up-triangles are from the results of  $K_xC_{60}$  reported by Duclos et al. (Ref.5), and down-triangles refer to the results of  $KBa_2C_{60}$  and  $KBaCsC_{60}$  reported by Yildirim et al. (Ref.16).

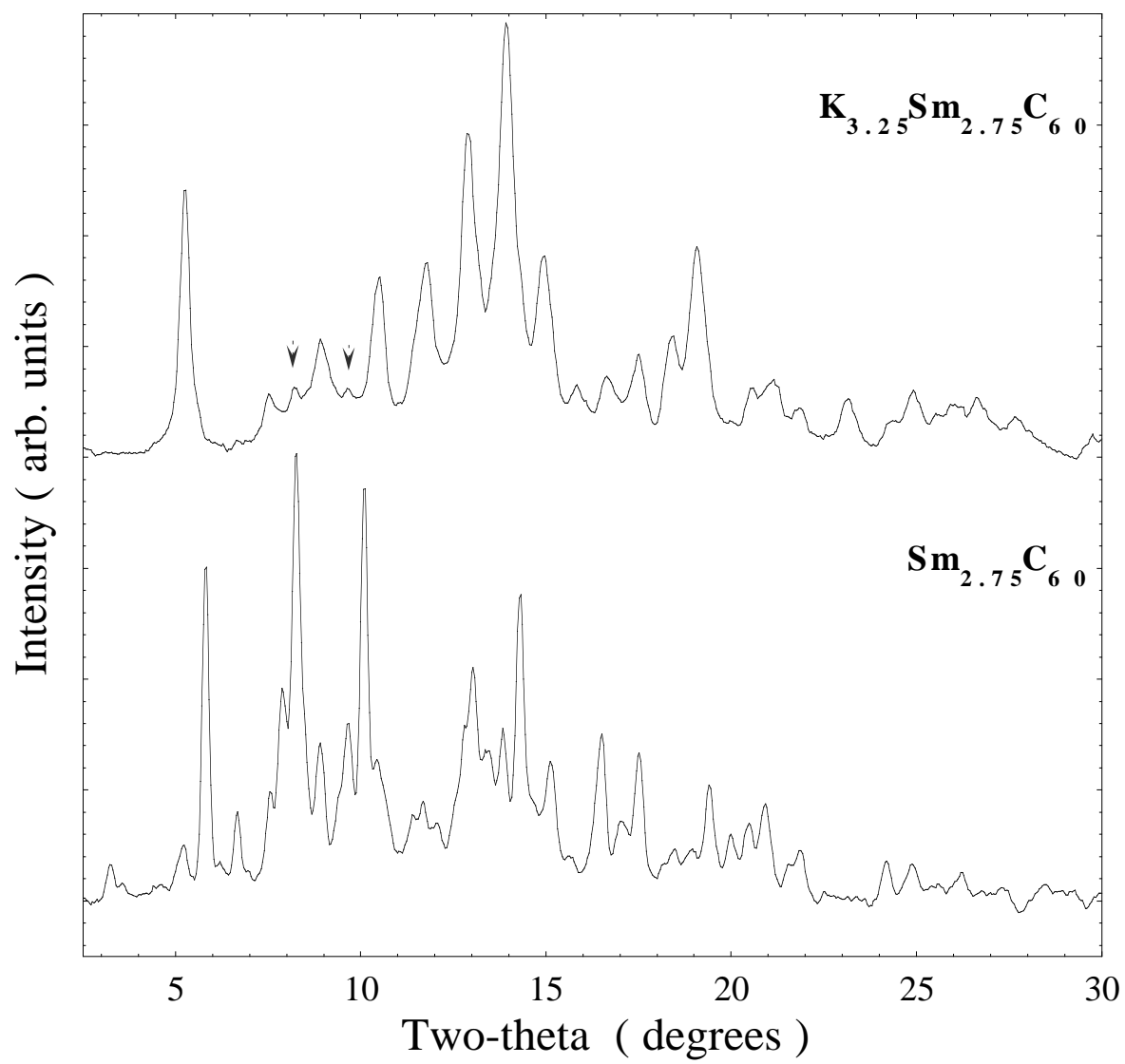


Fig.1

X. H. Chen et al.

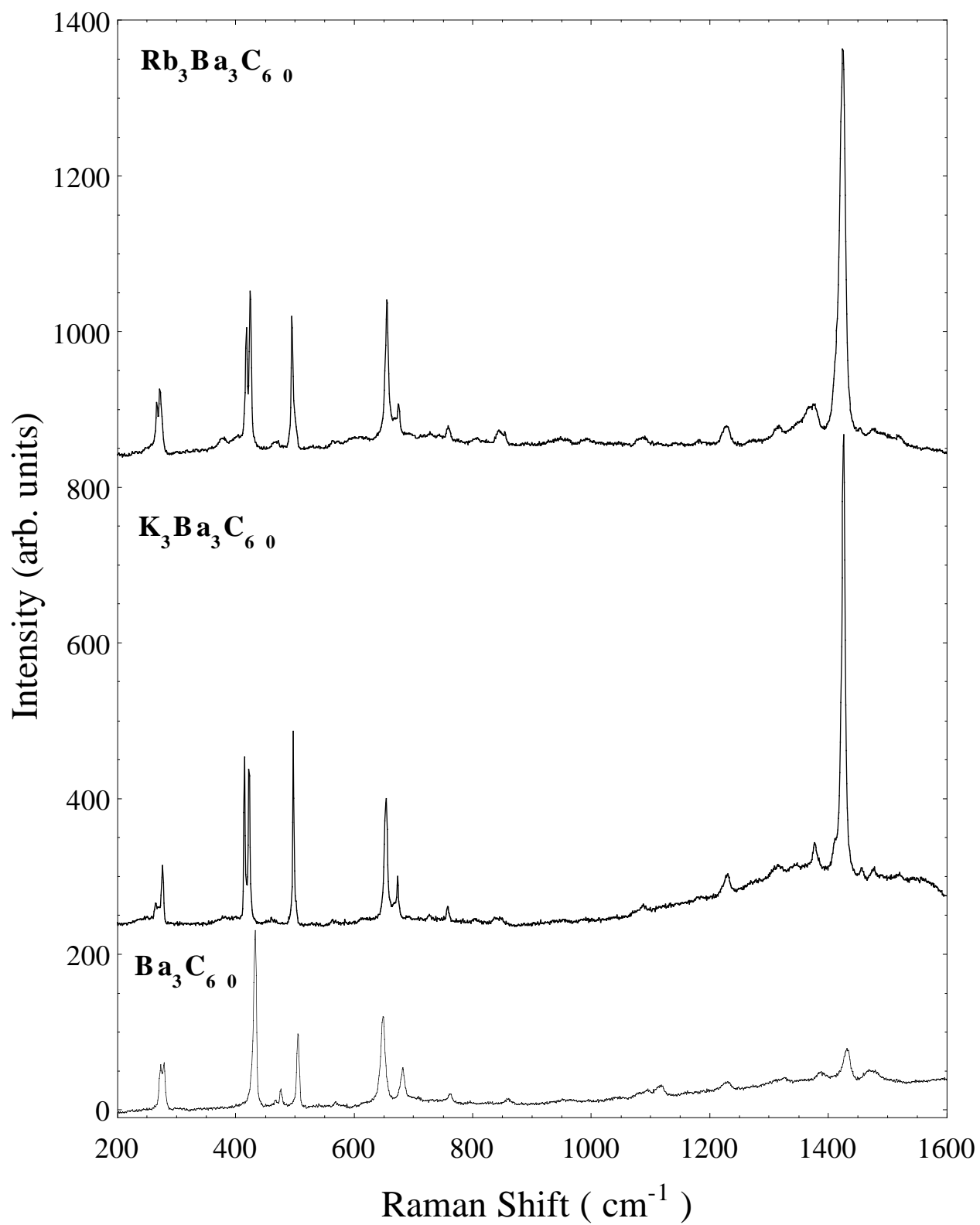


Fig.2

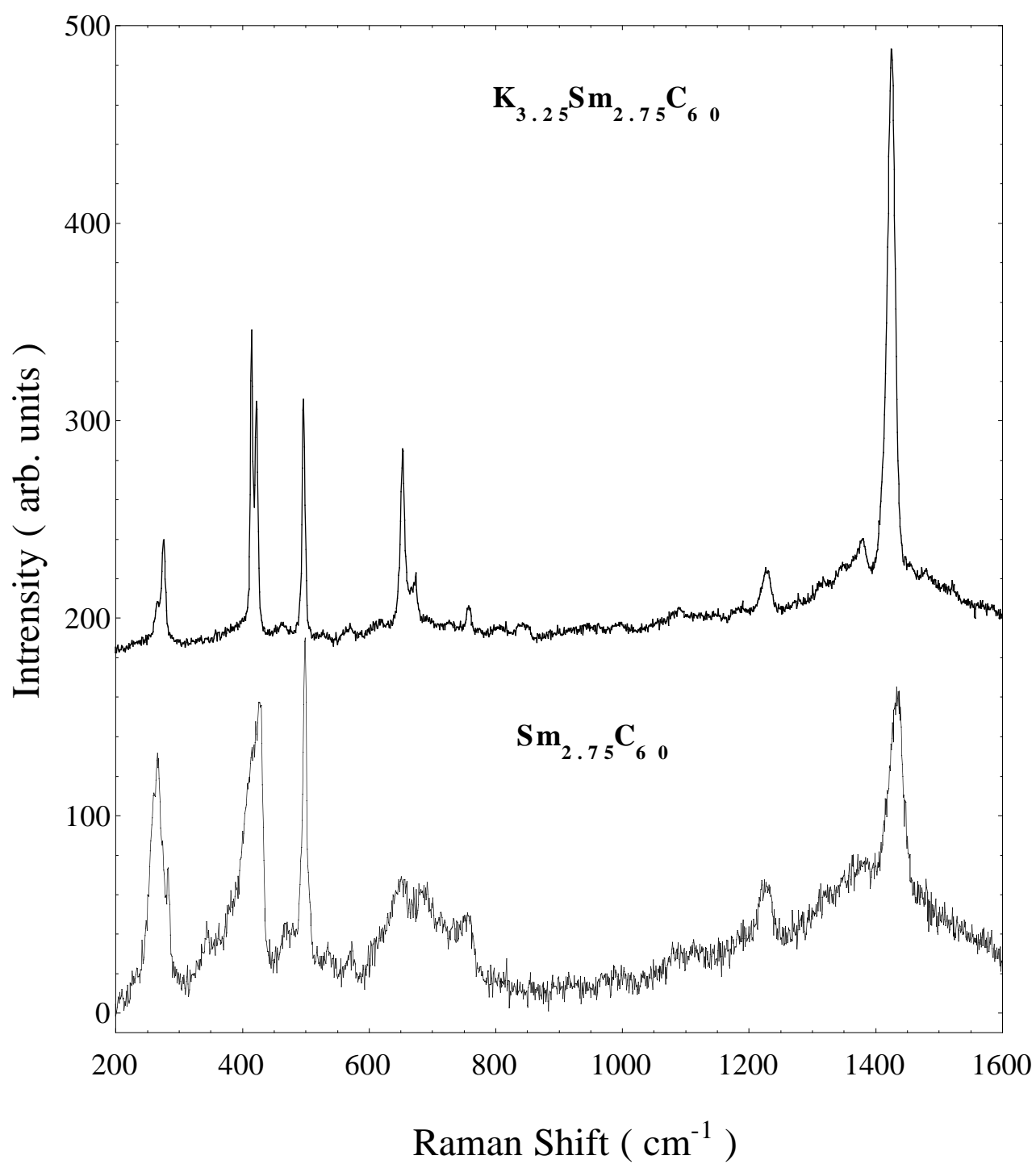


Fig.3

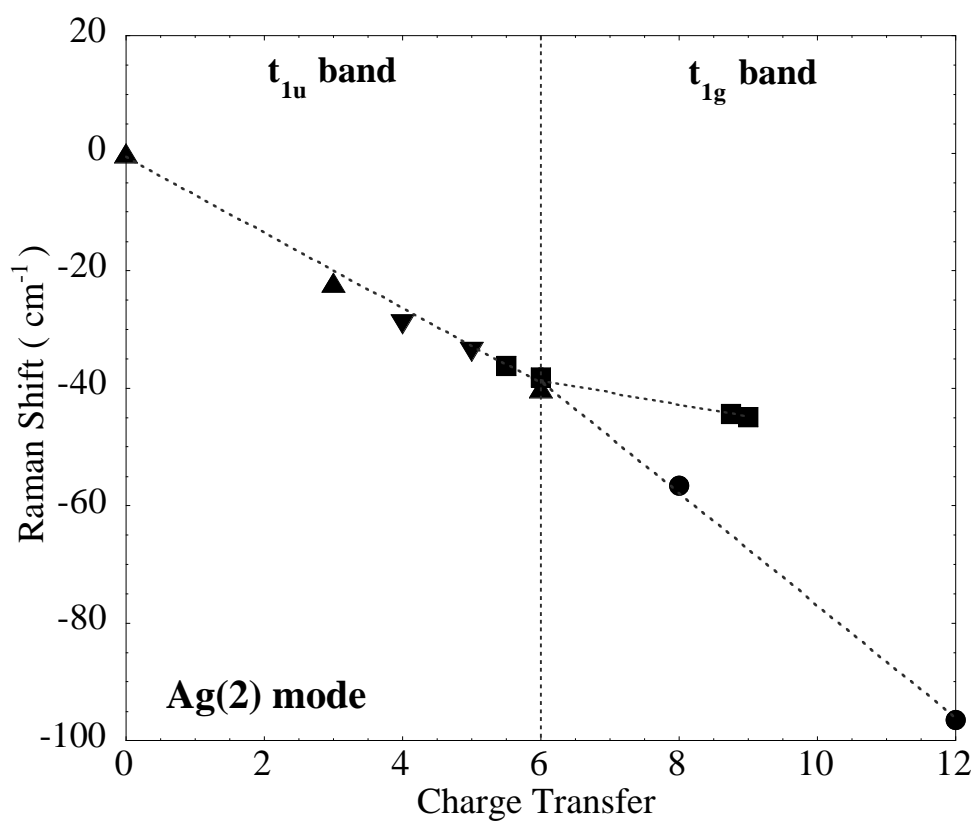
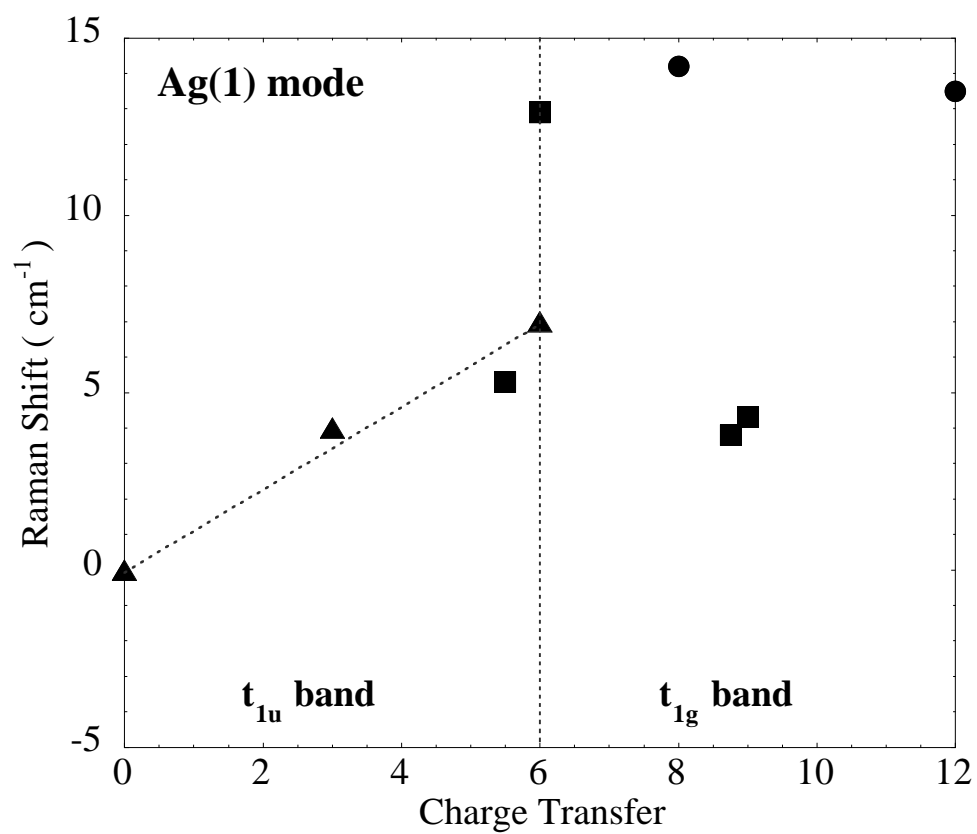


Fig.4